Journal of Peptide Science
J. Pept. Sci. 2008; **14**: 714–724
Published online 31 January 2008 in Wiley InterScience (www.interscience.wiley.com). DOI: 10.1002/psc.987

JOURNAL OF PEPTIDE SCIENCE

Kinetic and conformational properties of a novel T-cell antigen receptor transmembrane peptide in model membranes

MICHAEL A. AMON,[a] MARINA ALI,[a] VERONIKA BENDER,[a] KRISTOPHER HALL,[b] MARIE-ISABEL AGUILAR,[b] JANICE ALDRICH-WRIGHT[c] and NICHOLAS MANOLIOS[a]*

[a] Rheumatology Department, Westmead Hospital, Westmead, NSW, 2145, Australia
[b] Department of Biochemistry and Molecular Biology, Monash University, Clayton, VIC, 3800, Australia
[c] School of Biomedical and Health Sciences, College of Health & Sciences, University of Western Sydney, Penrith South DC, NSW, 2560, Australia

Received 7 August 2007; *Revised 10 October 2007*; *Accepted 25 October 2007*

Abstract: Core peptide (CP; GLRILLLKV) is a 9-amino acid peptide derived from the transmembrane sequence of the T-cell antigen receptor (TCR) α-subunit. CP inhibits T-cell activation both *in vitro* and *in vivo* by disruption of the TCR at the membrane level. To elucidate CP interactions with lipids, surface plasmon resonance (SPR) and circular dichroism (CD) were used to examine CP binding and secondary structure in the presence of either the anionic dimyristoyl-L-α-phosphatidyl-DL-glycerol (DMPG), or the zwitterionic dimyristoyl-L-α-phoshatidyl choline (DMPC).

Using lipid monolayers and bilayers, SPR experiments demonstrated that irreversible peptide–lipid binding required the hydrophobic interior provided by a membrane bilayer. The importance of electrostatic interactions between CP and phospholipids was highlighted on lipid monolayers as CP bound reversibly to anionic DMPG monolayers, with no detectable binding observed on neutral DMPC monolayers.

CD revealed a dose-dependent conformational change of CP from a dominantly random coil structure to that of β-structure as the concentration of lipid increased relative to CP. This occurred only in the presence of the anionic DMPG at a lipid : peptide molar ratio of 1.6 : 1 as no conformational change was observed when the zwitterionic DMPC was tested up to a lipid : peptide ratio of 8.4 : 1. Copyright © 2008 European Peptide Society and John Wiley & Sons, Ltd.

Keywords: circular dichroism; peptide; surface plasmon resonance; T-cell receptor

INTRODUCTION

The T-cell antigen receptor (TCR) is a critical component of the immune system able to recognize foreign antigens and to initiate the immune response. The TCR itself is a multi-subunit structure composed of at least seven transmembrane proteins. The TCR α and β chains are responsible for antigen recognition, and the associated CD3 chains, γ, δ, ε, and ζ, are responsible for the ensuing signal transduction required to initiate cellular activation and subsequent immune response. An analysis of TCR structure reveals the presence of at least one charged amino acid within each subunit's transmembrane region. While the TCR α and β chains contain two and one positive residues respectively, the CD3 chains possess one negative amino acid, each of which are essential for TCR assembly and function [1–5]. Previous work regarding the importance of the transmembrane region in assembly has led to the discovery of a 9-amino acid peptide, termed core peptide (CP), capable of inhibiting T-cell activation both *in vitro* and *in vivo* [6–12]. The sequence of CP, GLRILLLKV, is a copy of the 9-amino acid sequence within the TCR α-transmembrane domain containing two positively charged residues, arginine and lysine. These two positively charged residues have been shown to be essential for assembly of the TCR α with the CD3 $\delta\varepsilon$ and CD3 $\zeta\zeta$ signaling oligomers [1,4,5,13].

Previous investigations on CP have focused on determining CP's cellular specificity [14], peptide–protein interactions [6–8], and the effect of CP on different models of T-cell mediated disease [8–12]. To date, few results have been published concerning CP's biophysical properties [15–17]. Ali *et al.* first reported CP interactions with membranes by EM, ^{31}P and ^{2}H solid-state NMR spectroscopy, and CD [16]. This paper reported that CP did not form pores within the cell's membrane, but was capable of disrupting model membrane vesicles, at high peptide concentrations [16]. Using NMR experiments and the zwitterionic dimyristoyl-L-α-phoshatidyl choline (DMPC), or a 1 : 3 molar mixture of the anionic dimyristoyl-L-α-phosphatidyl-DL-glycerol DMPG and DMPC liposomes, Ali *et al.* demonstrated that CP was capable of disrupting membrane vesicles at high peptide concentrations, and that this perturbation was related to lipid charge [16]. At high peptide concentration, CP did little to disrupt the DMPC bilayer, whereas in bilayers composed of DMPG : DMPC (1 : 3), CP formed an amorphous aggregate structure [16]. CD,

*Correspondence to: Nicholas Manolios, Rheumatology Department, Westmead Hospital, Westmead, NSW, 2145, Australia;
e-mail: nickm@westgate.wh.usyd.edu.au

which has been used extensively to determine the secondary conformation of various peptides in different environments [16,18–21], was then used to examine CP secondary-structure elements. In the presence of water, CP presented as essentially random coil with some alpha helix, and remained as such in the presence of DMPC, even at high peptide : lipid ratios [16]. In TFE, a solvent commonly used to observe peptides and proteins in a hydrophobic milieu and known to stabilize helix formation [22,23], the amount of α-helix increased significantly. By contrast, in the presence of DMPG liposomes, CP was found essentially in β-structure [16].

To further examine CP's relationship to lipid membranes, Bender *et al.* used surface plasmon resonance (SPR) and demonstrated a strong correlation between CP's ability to bind to model membranes and CP's ability to inhibit T-cell activation *in vitro* [17]. While a kinetic analysis of peptide binding was beyond the scope of this initial study, Bender *et al.* proposed that CP's ability to bind to membranes was probably dependent upon the charged amino acids arginine and lysine, since any alteration or removal of the basic residues significantly reduced CP's ability to bind to lipid bilayers [17]. It was also noted that there was a quantitative difference in CP binding depending on the type of lipid used [17]. Upon dissociation, CP was observed to be retained to a greater degree in the anionic DMPG bilayer than to the zwitterionic DMPC, suggesting an important role for lipid charge in CP–lipid interactions [17].

The present study aims at extending these previous studies and further define the interactions occurring between CP and the anionic DMPG or zwitterionic DMPC lipids. CP–lipid interactions are initially investigated by SPR to examine CP binding to anionic and zwitterionic membrane monolayers and bilayers. CD is then employed to examine the conformational changes undergone by CP as a direct result of lipid vesicle addition, which may facilitate insertion or retention within membranes.

MATERIALS AND METHODS

Materials

DMPC, DMPG, and *N*-octyl- β-D-glucopyranoside were purchased from Sigma (St.Louis, MO, USA). Pioneer L1 and HPA chips were purchased from Biacore (Uppsala, Sweden).

CP was synthesized by manual Fmoc solid-phase chemistry and purified using a Vydac C18 reverse-phase column on an Agilant 1100 series HPLC and characterized by electrospray spectrometry. CP was dissolved in milliQ water as 1 mM stock solutions and serially diluted with *N*-2-hydroxyethylpiperazine-*N*-2-ethanesulfonic acid (HEPES) buffered saline (HBS-N; 0.88% NaCl) as supplied by BIAcore prior to analysis by SPR, and to 250 μM and 100 μM in milliQ water for analysis by CD. CP was also dissolved in phosphate buffered saline (PBS, pH 7.2) to a concentration of 100 μM for CD analysis.

Preparation of Small Unilamellar Vesicles (SUVs)

For SPR analysis, DMPC and DMPG lipids were dissolved in dry chloroform and chloroform/methanol (2 : 1), respectively, to give 10 mg/ml solutions. These were evaporated under reduced pressure and the resulting lipid films dried overnight *in vacuo*. Lipids were hydrated by resuspending in HEPES for 60 min at 34 °C to give 0.5 mM concentration in respect of phospholipids. The solutions were subsequently sonicated in an ultrasonic bath for 20 min. Small unilamellar vesicles (SUVs) were created with eight freeze/thaw cycles followed by extrusion with a Liposofast apparatus (Avestin, Ottawa, Canada) through polycarbonate filters of firstly 100 nm pore diameter with 21 passages, and secondly of 50 nm pore diameter with 21 passages [17]. Liposomes were immediately applied to sensor chips for SPR analysis. For CD analysis, DMPG (and DMPC) lipid films were prepared as above and subsequently hydrated to 2 mM in milliQ water or PBS by sonication with a Branson tip sonicator until clear.

Binding Analysis by Surface Plasmon Resonance

SPR was carried out on a BIAcore 2000 instrument using a Pioneer Sensor Chip L1 to analyze peptide binding to membrane bilayers [24,25], and with an HPA chip to analyze peptide binding to supported lipid monolayers [24,25]. The L1 sensor chip is composed of a modified dextran matrix on a gold surface capable of maintaining a lipid bilayer environment [24,25]. The HPA sensor chip is composed of long-chain alkanethiol molecules covalently linked to a gold surface designed to allow the production of a hybrid bilayer membrane, or supported lipid monolayer [24,25]. Running buffer was a 10% mixture of milliQ water in HBS-N.

SPR sensorgrams for kinetic analysis were acquired using previously-established protocols described by Aguilar [21,26–29] and Shai [24]. Briefly, the chip surfaces were cleaned with 40 mM octyl glycoside (40 μl, 10 μl/min) followed by running buffer (5 μl/min) until a stable baseline was achieved. Membrane bilayers were formed on the L1 chip by injecting 100 μl of liposomes (SUVs) at a flow rate of 5 μl/min, followed by a 10 mM NaOH wash (30 μl, 10 μl/min) to remove any multilamellar vesicles from the surface of the sensor chip. The flow was then set to 5 μl/min. Upon achieving a stable baseline, 150 μl of peptide was injected at a flow rate of 5 μl/min and allowed to dissociate from the membrane for not less than 2000 s. Peptides tested ranged in concentration from 5 to 50 μM in 10% milliQ water in HBS-N buffer. Regeneration of the sensor chip was achieved with 40 mM β-octylglycoside (30 μl, 10 μl/min). For experiments performed on the HPA chip, monolayers were formed by injecting 250 μl of extruded liposomes at a flow rate of 2 μl/min, followed by a 10 mM NaOH wash consisting of 30 μl at a flow rate of 10 μl/min. The flow rate was then set to 5 μl/min for analysis of peptide binding (conditions as per L1 chip). All SPR experiments were run at 25 °C.

One of the difficulties encountered with CP binding to membrane bilayers was the irreversible binding mentioned in the introduction [17]. This phenomenon, which has been observed for other peptides [29], was again observed herein such that a dissociation phase extending over 18 h failed to approach baseline levels (data not shown). This resulted in an inability to reuse the same lipid bilayer for different peptide

DOI: 10.1002/psc

concentrations during the kinetic analysis. Consequently, each flow-cell was stripped and a new lipid layer formed before a different peptide concentration could be tested. To be included in this analysis, the immobilized lipid content measured in response unit (RU) was as close as possible for each peptide concentration tested, resulting in average lipid contents of 6529 RU ±4% for DMPC bilayers, and 4801 RU ±20% for DMPG bilayers (error is in standard deviation). Kamimori *et al.* have reported that a minimum level of approximately 4500 RUs allows reproducible results in peptide–lipid binding sensorgrams [30]. A similar finding was observed here as identical peptide concentrations resulted in identical sensorgrams when examined on lipid bilayers of 5636 and 6413 RU (data not shown).

The sensorgrams obtained from each peptide–lipid interaction were analyzed using the BIAevaluation software version 4.1 software as supplied by BIAcore. Data was initially fit separately using BIAevaluation 4.1 to produce apparent association ($k_a$app) and dissociation ($k_d$app) rate constants for each data set (DMPG on L1 and HPA sensor chips, and DMPC on the L1 sensor chip). The apparent dissociation rate ($k_d$app) was calculated by fitting the dissociation data for each data set globally. The resulting $k_d$app was then used to solve for $k_a$app by globally fitting the association data. Data points used for the analysis were chosen based on regions where the plot of dR/dt *versus* time for all the data sets were constant, representing regions with a constant rate of change of RU with respect to time (500–1800 s for association, 2500–3500 s for dissociation). $K_A$app and $K_D$app were calculated as $k_a$app/$k_d$app and $k_d$app/$k_a$app, respectively. The observed rate constant ($k_{obs} = k_a\text{app}^*[\text{CP}] + k_d\text{app}$) *versus* [CP] was plotted to further assess the quality of each fit. This plot is expected to be linear with a slope equal to the $k_a$app, and the y-intercept equal to $k_d$app [31].

Association and dissociation data were subsequently fit to the supplied simultaneous binding models where association and dissociation data sets are fit at the same time (parallel reaction model, two-state reaction model, 1 : 1 Langmuir model). Improved fits were only observed when sensorgrams resulting from CP binding to DMPG on the L1 sensor chip to the two-state reaction model were examined. The two-state reaction model describes a peptide–lipid interaction based on the model:

$$\text{P} + \text{L} \underset{k_{d1}}{\overset{k_{a1}}{\rightleftharpoons}} \text{PL} \underset{k_{d2}}{\overset{k_{a2}}{\rightleftharpoons}} \text{PL}^*$$

In this model, P represents the peptide (CP), L represents the lipid (either DMPC or DMPG), and PL is a peptide–lipid complex theoretically formed by the electrostatic interactions between P(CP) and the lipid (L). PL* is a complex which is incapable of dissociating directly to the individual P and L components. PL* is proposed to correspond to the membrane-insertion step whereby P(CP) is inserted into the membrane layer L [21]. The affinity constant for the initial electrostatic interaction (K_1) is calculated from the rate constants as k_{a1}/k_{d1}, and the affinity constant for the predicted membrane-insertion step (K_2) is k_{a2}/k_{d2}. The overall affinity constant (K) is calculated as $(k_{a1}/k_{d1}) \times (k_{a2}/k_{d2})$.

Circular Dichroism

CD spectra were measured in a 0.1 cm quartz cuvette using a Jasco J-810 spectropolarimeter (Jasco Corp., Tokyo, Japan). Spectra were recorded from 250 to 190 nm at a sensitivity of 100 mdeg, a resolution of 0.5 nm, a response of 1 s, a bandwidth of 1.0 nm, and a scan speed of 100 nm/min, with 30 accumulations. Peptide solutions were prepared by dissolving CP at 250 μM in milliQ water, or 100 μM in PBS (pH 7.2). Higher concentrations were not possible in PBS as precipitation was visible. Concentrations were chosen so as to provide as strong a signal as possible for spectra acquisition.

DMPG (or DMPC) at 2 mM was progressively added to 200 μl of CP (250 μM in milliQ water, or 100 μM in PBS) and allowed to stand at room temperature for 10 min prior to spectrum acquisition. Spectra background were corrected prior to analysis. Data was analyzed using the 'PEPFIT Analysis' software, which was developed based on the original PEPFIT program of Reed *et al.* [32], now modified to work within Microsoft Excel, and available through the authors. PEPFIT Analysis estimates secondary structure by fitting experimental data to reference secondary structure spectra whereby the best fit is defined using the R^2 value, where an R^2 value equal to one is defined as a perfect fit.

RESULTS

Membrane Binding Affinity of CP Analyzed by SPR

CP binding to membrane bilayers. Upon CP binding to DMPG and DMPC bilayers (Figure 1), the most notable difference was the RU levels reached during the association phase (0–1800 s), as the resulting RUs at 1800 s on DMPG were approximately twice that obtained when CP was analyzed on DMPC. On both lipid bilayers, CP presented with a rapid association phase, and significant irreversible binding following the dissociation phase (>1800 s).

Apparent kinetic constants were determined by fitting each data set globally and calculating the association and dissociation constants separately to produce apparent rate ($k_a$app and $k_d$app) and affinity ($K_A$app and $K_D$app) constants. Also produced were k_{obs} values which, when plotted against CP concentration, provide an assessment of the quality of the fit (Figure 1(c) and (d)). The plot of k_{obs} *versus* CP concentration should result in a straight line with a slope of $k_a$app and a y-intercept of $k_d$app [31]. The resulting kinetic constants, presented in Table 1, suggested that CP bound to anionic DMPG bilayers at a faster rate than to zwitterionic DMPC bilayers ($k_a$app = 32.8 vs 23.9 respectively). Upon dissociation however, CP dissociates from DMPC at a rate approximately five-fold slower than from its DMPG counterpart. Examination of the sensorgrams between 2000 s and 3500 s suggest that the higher $k_d$app observed on DMPG bilayers was the result of a well-defined negative slope throughout this region in DMPG sensorgrams. During CP dissociation from DMPC however, only a slight negative slope from 2000 to 3500 s was observed, indicating that very little peptide was dissociating from the membrane. The affinity constants of each lipid

DOI: 10.1002/psc

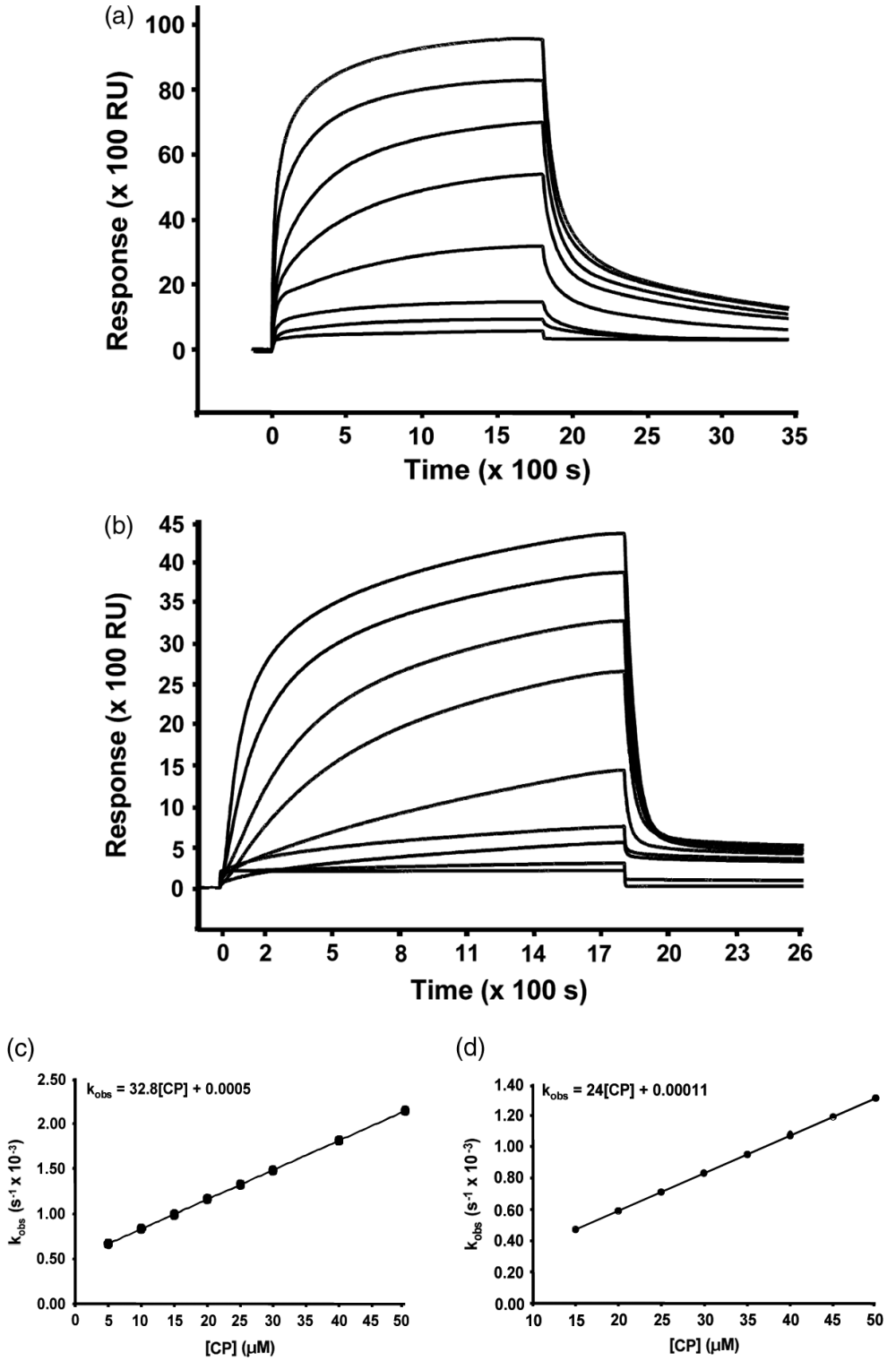

Figure 1 Sensorgrams showing core peptide(CP) binding to lipid bilayers on the L1 sensor chip surface composed of either (a) DMPG or (b) DMPC. Core peptide concentrations range from 5 μM (DMPG) or 10 μM (DMPC) to 50 μM. Data is presented in response units (RU). Plot of observed rate constant (k_{obs}) *versus* CP concentration used to asses the fit obtained by separately determining $k_d$app and $k_a$app for bilayers composed of either DMPG (c) or DMPC (d) as described in the 'Materials and Methods' Section. Apparent association ($k_a$app) and dissociation rate ($k_d$app) constants can be determined from the slope and intercept, respectively as $k_{obs} = (k_a\text{app}) \times [\text{CP}] + k_d\text{app}$ [31]. This curve is expected to be linear across the range of concentrations tested.

bilayer further suggested an approximately three-fold higher affinity for DMPC than for DMPG ($K_A$app = 21.6×10^4 vs 6.58×10^4 M^{-1}, respectively), likely driven by the lower $k_d$app for CP binding to DMPC bilayers.

DOI: 10.1002/psc

The kinetic estimations presented in Table 2 were evaluated based on the two-state reaction model. This model predicts that the first step in peptide binding is based on electrostatic interactions between the peptide and phospholipid head groups, where the rate of association is given by k_{a1}, and the rate of dissociation is given by k_{d1}. The affinity constant, K_1, for the proposed electrostatic interaction is calculated as k_{a1}/k_{d1}. The second step is predicted to be the membrane-insertion step, as mediated by the hydrophobic interactions between peptide and the membrane interior (k_{a2}, k_{d2}), with an affinity constant of K_2 calculated by k_{a2}/k_{d2}. The affinity constant for the entire binding process, K, is determined as $(k_{a1}/k_{d1}) \times (k_{a2}/k_{d2})$.

The two-state reaction model is currently the proposed model for amphipathic membrane-active peptides [24,25,28,33]. However, as noted by others, despite the acceptance of the two-state model and its improved fits, it is possible that CP (and other amphipathic peptides) may bind to lipids in a more complex fashion than the few models currently available in the BIAevaluation 4.1 software allow for [27,28]. Surprisingly, only data from CP interactions with DMPG bilayers produced acceptable fits using the two-state model, suggesting that CP may interact with different lipids via more complex mechanisms. The kinetic constants calculated using the two-state model (presented in Table 2) predict that electrostatic interactions between the peptide, and the lipid drove the observed binding events. The k_{a1} for the electrostatic interactions was 80.1 $M^{-1}s^{-1}$ whereas the dissociation rate constant (k_{d1}) was 0.00727 s^{-1}, to produce an affinity constant for the initial electrostatic interaction step (K_1) of 1.1×10^4 M^{-1} whereas the membrane-insertion step resulted in an affinity constant (K_2) of 0.92.

CP binding to membrane monolayers. To examine the importance of the membrane bilayer in CP–lipid interactions, CP binding to supported DMPG or DMPC lipid monolayers was analyzed. The technique of analyzing peptide–lipid binding to lipid monolayers supported with the HPA chip *versus* bilayers formed on the L1 chip has recently been used by others to examine peptide interactions with different lipid membrane systems [24,34]. Papo and Shai recently used this approach to differentiate between the carpet-forming magainin and the transmembrane pore-forming melittin [24]. It was proposed that by using both monolayers and bilayers, differentiation between membrane-surface binding and membrane insertion can be accomplished by allowing a direct examination of the effect of the membrane bilayer during peptide binding. By comparing the affinity constants derived from magainin and melittin binding to monolayers and bilayers, it was demonstrated that magainin was not significantly influenced by the membrane's inner layer. Furthermore, it was observed that the $K_A$bilayer : $K_A$monolayer ratio for melittin on lipid layers composed of phosphatidyl choline : cholesterol (10 : 1 w/w) was 25, suggesting that melittin was heavily reliant upon the hydrophobic interior provided by the membrane

Table 1 Apparent kinetic constants of CP binding to DMPG or DMPC bilayers (L1 chip) or monolayers (HPA chip) derived from a pseudo first-order reaction mechanism[a]

Lipid	Layer	$k_a$app ($M^{-1}s^{-1}$)	SE $k_a$app	$k_d$app ($s^{-1} \times 10^{-4}$)	SE $k_d$app ($\times 10^{-6}$)	$K_A$app ($M^{-1} \times 10^4$)	$K_D$app ($M \times 10^{-5}$)	$K_A$app bilayer/$K_A$app monolayer
DMPG	Bi	32.8	0.194	4.99	1.23	6.58	1.52	1.92
DMPG	Mono	27.3	0.147	7.99	3.16	3.42	2.93	
DMPC	Bi	23.9	0.105	1.11	0.535	21.6	0.464	NA
DMPC	Mono	—	—	—	—	—	—	

[a] $K_A$app represents the apparent affinity constant for the complete binding reaction and was derived as ($k_a$app/$k_d$app). $K_D$app represents the apparent dissociation constant for the complete binding reaction and was derived as ($k_d$app/$k_a$app).

Table 2 Kinetic constants of CP binding to DMPG bilayers on the L1 chip derived from the two-state reaction model[a]

Lipid	k_{a1} ($M^{-1}s^{-1}$)	SE k_{a1}	k_{d1} ($s^{-1} \times 10^{-3}$)	SE k_{d1} ($\times 10^{-5}$)	K_1 ($M^{-1} \times 10^4$)	k_{a2} ($s^{-1} \times 10^{-4}$)	SE k_{a2} ($\times 10^{-6}$)	k_{d2} ($\times 10^{-4}$)	SE k_{d2} ($\times 10^{-6}$)	K_2	K ($M^{-1} \times 10^4$)
DMPG	80.1	1.03	7.27	8.97	1.11	5.75	7.29	6.24	7.03	0.92	2.12

[a] The affinity constants K_1 and K_2 were determined for the first and second peptide–lipid binding steps respectively and were determined as $K_1 = k_{a1}/k_{d1}$ and $K_2 = k_{a2}/k_{d2}$. K is determined as $(k_{a1}/k_{d1}) \times (k_{a2}/k_{d2})$ and represents the affinity constant for the entire binding process.

DOI: 10.1002/psc

bilayer as opposed to the pseudobilayer provided by the HPA chip [24].

Presently, a similar analysis and method was employed to examine CP binding to different monolayers prepared on the HPA sensor chip. Figure 2 shows the results obtained when CP was examined in the presence of monolayers composed of either DMPG or DMPC. Using this system, it was hypothesized that CP's ability to insert into the hydrophobic interior would be significantly hindered as the HPA chip provides a supported lipid monolayer which offers restricted membrane insertion of peptides and proteins [25].

CP binding to DMPG monolayers demonstrated less pronounced binding than that observed through the use of bilayers as indicated by the RU values. At 1800 s, CP binding to DMPG monolayers resulted in 3000 RU, whereas CP binding to DMPG bilayers resulted in 9500 RU, an approximately three-fold difference. Furthermore, CP binding to DMPG monolayers was reversible, such that each sensorgram obtained at each peptide concentration returned to baseline after approximately 3 h, meaning that the same liposome surface could be reused for each peptide concentration.

During the kinetic analysis, it was noted that none of the supplied models for simultaneously fitting association and dissociation phases within the BIAevaluation 4.1 software were able to result in a satisfactory fit. Using the same analysis method described for the bilayer systems, apparent kinetic constants were then calculated and are presented in Table 1. Interestingly, the apparent association rate constant ($k_a$app) for CP on DMPG monolayers is approximately the same as that observed on DMPG bilayers (27.3 and 32.8 $M^{-1}s^{-1}$, respectively), suggesting that the association rate of CP was not dependent upon the presence of a lipid bilayer. The apparent dissociation rate constant observed for CP on DMPG monolayers was approximately 60% higher than that observed for CP binding to DMPG bilayers (7.99×10^{-4} and 4.99×10^{-4} s^{-1}, respectively). While this is not a large difference, it may account for the lower RUs observed on DMPG monolayers when compared to bilayers.

Shai and colleagues have shown that a comparison of the affinity constants obtained for peptide binding to monolayers and bilayers can provide an indication of the contribution of the inner leaflet in the peptide–lipid binding process [24]. This value, given by the ratio $K_A$bilayer/$K_A$monolayer in Table 1, for DMPG was 1.92, indicating that CP was only marginally influenced by the hydrophobic interior provided by the DMPG bilayer formed on the L1 sensor chip.

Upon binding to zwitterionic DMPC monolayers, while weak association may be present, dissociation was too fast to permit a kinetic analysis (Figure 2). While no kinetic information could be obtained from this result, it was nonetheless an important observation as it suggests that the weak initial association between CP and DMPC is driven forward by the subsequent interactions between CP and the hydrophobic interior of the inner leaflet of the membrane bilayer.

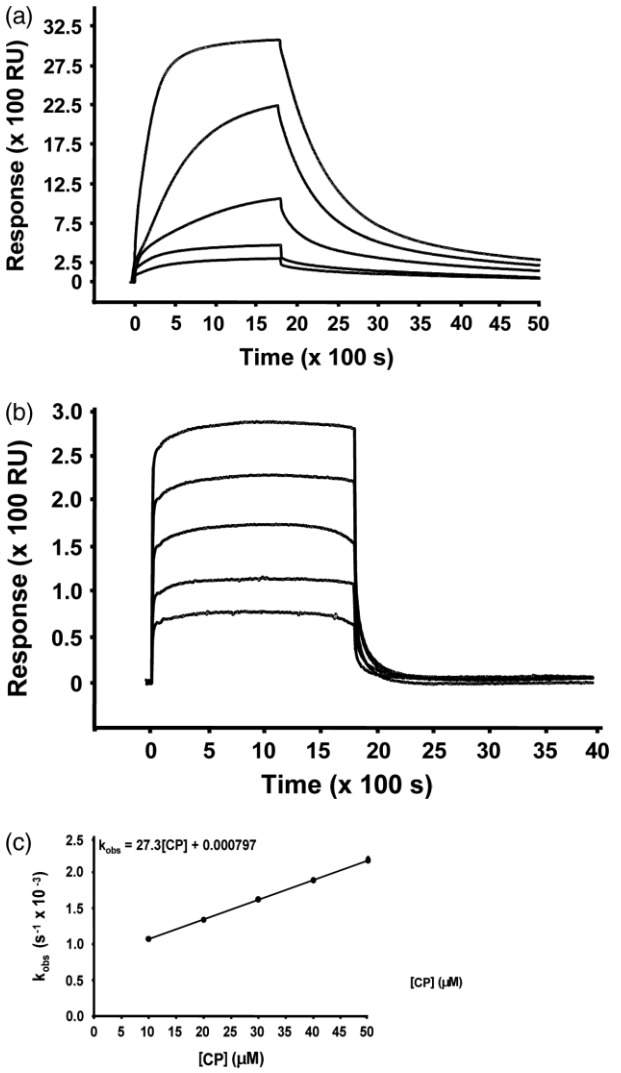

Figure 2 Sensorgram showing Core Peptide(CP) binding to lipid monolayers on the HPA sensor chip composed of either (a) DMPG, or (b) DMPC. CP concentrations range from 10 to 50 μM. Data is presented in response units (RU). Plot of observed rate constant (k_{obs}) *versus* CP concentration used to assess the fit obtained by separately determining $k_d$app and $k_a$app for monolayers composed of DMPG (c) as described in the 'Materials and Methods' Section. Apparent association ($k_a$app) and dissociation rate ($k_d$app) constants can be determined from the slope and intercept, respectively as $k_{obs} = (k_a\text{app}) \times [\text{CP}] + k_d\text{app}$ [31]. This curve is expected to be linear across the range of concentrations tested.

CP secondary structure assessed by CD. Secondary structure analysis of CP at various lipid : peptide molar ratios was examined using CD in the presence of DMPG or DMPC in either PBS or milliQ water and subsequently analyzed using the PEPFIT Analysis program. The PEPFIT Analysis program, which runs

DOI: 10.1002/psc

within Microsoft Excel, is entirely based on the MS-DOS based operator-intervention fitting program entitled PEPFIT as created by Reed *et al.* [32]. Using R_2 values to produce best fits between experimental data and published reference spectra, PEPFIT Analysis greatly reduces the potential bias resulting from the operator-intervention format of the original PEPFIT program [32]. Standard CD deconvoluting software, such as CDPro and Dichroweb [35], were not employed as they generally use globular proteins as reference sets, and were therefore deemed inappropriate in the analysis of CP, which is a small molecular weight, hydrophobic transmembrane peptide.

CP secondary structure in milliQ water. The effects of lipid vesicles on CP secondary structure was investigated by incubating 250 μM CP with increasing amounts of either DMPG or DMPC lipids in milliQ water (Figure 3(a) and (b), respectively). In the absence of lipid, CP appears as predominantly random coil in milliQ water, and upon DMPG addition, undergoes

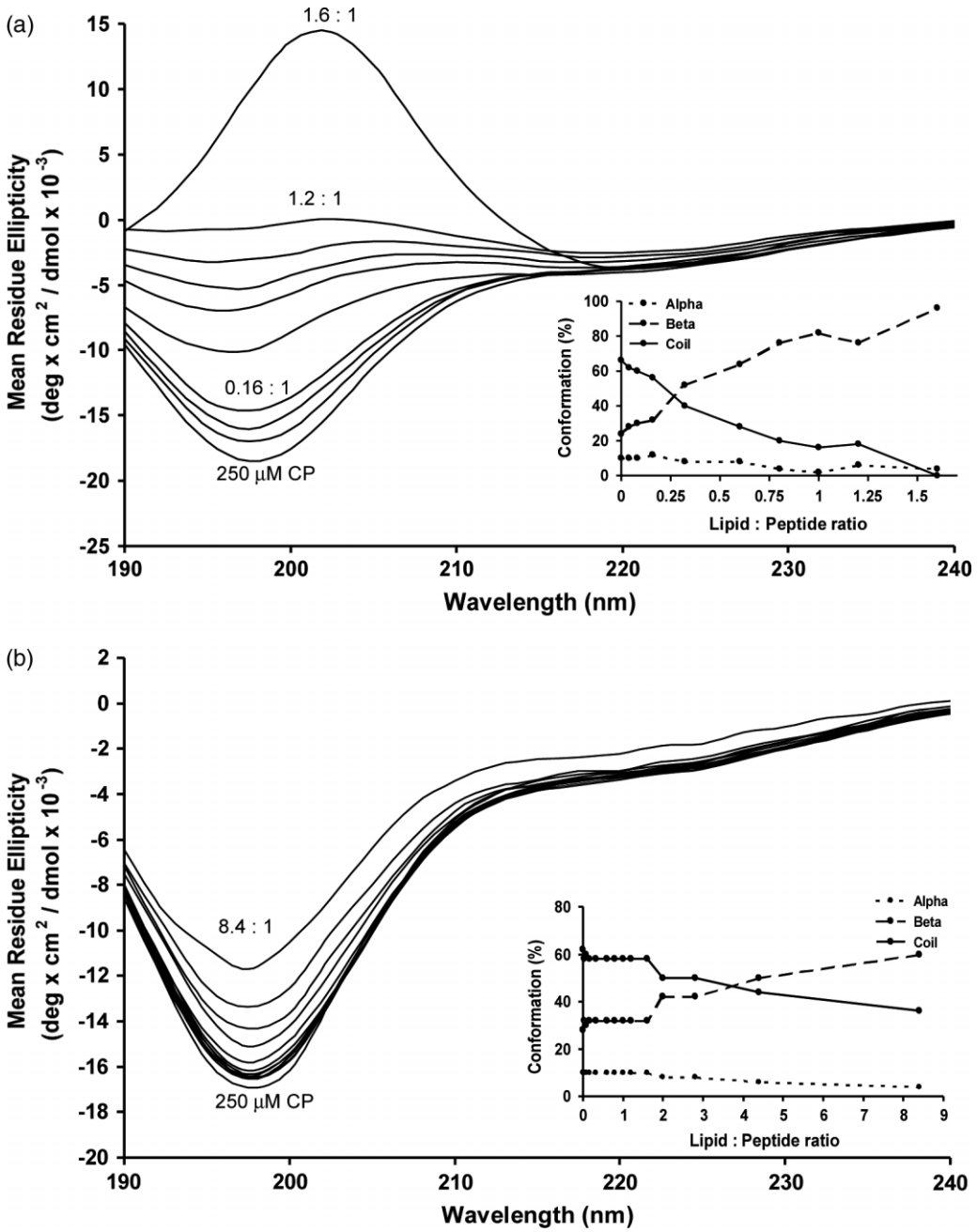

Figure 3 CD spectra of CP at 250 μM in milliQ water in (a) DMPG at lipid : peptide ratios of 0, 0.04, 0.08, 0.16, 0.32, 0.6, 0.8, 1.0, 1.2, and 1.6 : 1; and (b) in DMPC at lipid : peptide ratios of 0, 0.04, 0.08, 0.16, 0.32, 0.6, 0.8, 1.0, 1.2, 1.6, 2.0, 2.8, 4.4, and 8.4 :1. Insets show secondary structure content (%) as a function of lipid : peptide ratio calculated using the PEPFIT [32] derived PEPFIT Analysis software.

DOI: 10.1002/psc

a conformational change to an almost exclusively β-conformation (Figure 3(a), inset). In the presence of DMPC, CP does not appear to change conformation appreciably, with coil structure dropping from approximately 60% (250 μM CP alone) to 40% at a lipid : peptide molar ratio of 8.4 : 1 (Figure 3(b), insert).

CP secondary structure in PBS. To examine the effect of PBS on CP's lipid induced secondary structure, increasing amounts of either DMPG or DMPC in PBS were added to 100 μM CP also in PBS (Figure 4). In the absence of lipid, CP in PBS presents with approximately 60% β-structure and 40% coil. Upon addition of DMPG in PBS, CP's conformation changed to approximately 80% β-structure and 20% coil (Figure 4(a)). Addition of DMPC had no effect on CP secondary structure (Figure 4(b)). The spectral intensities of CP were considerably lower for DMPC than for DMPG, suggesting that most of the peptide may be in the form of insoluble aggregates when in the presence of DMPC vesicles. By contrast, the higher intensities and well-defined spectra observed in the presence of DMPG vesicles suggested that this anionic lipid is capable of interacting and inducing conformation changes with CP aggregates.

DISCUSSION

CP, a nonapeptide derived from the transmembrane region of the TCR α-chain, has previously been shown to inhibit T-cell activation *in vitro* as well as *in vivo*, with recent studies suggesting that CP disrupts signal transduction within the surface expressed

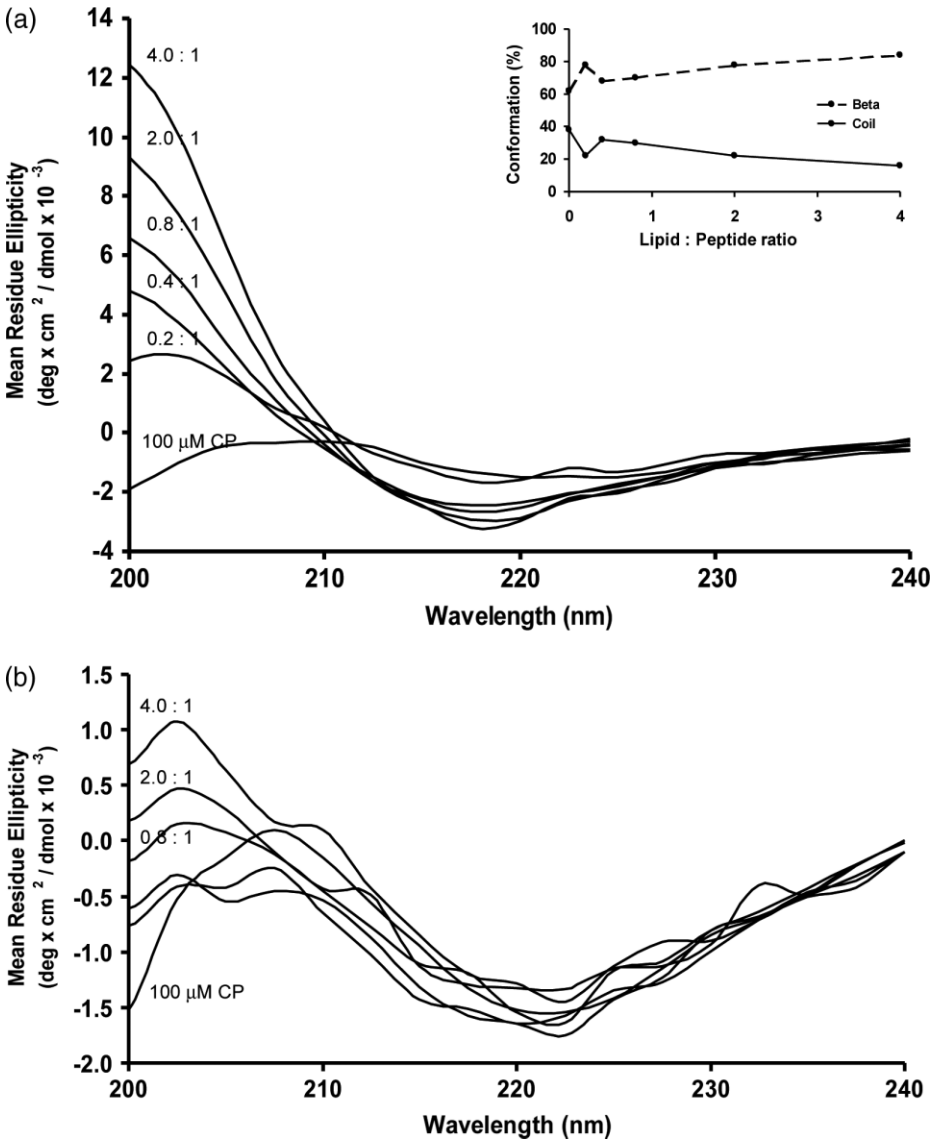

Figure 4 CD spectra of CP at 100 μM in PBS alone and at lipid : peptide ratios of 0, 0.2, 0.4, 0.8, 2.0, and 4.0 : 1 in (a) DMPG and (b) DMPC. Inset shows secondary structure content (%) as a function of lipid : peptide ratio calculated using the PEPFIT [32] derived PEPFIT Analysis software.

DOI: 10.1002/psc

TCR–CD3 complex [6–8,12,36,37]. Consequently, how CP interacts with lipid membranes is an essential facet of CP activity. In this study, CP–lipid interactions were initially assessed by kinetically examining CP's ability to bind to various artificial lipid membranes by SPR. CD was then used to examine the lipid–induced secondary structure of CP in the presence of increasing concentrations of DMPG or DMPC in either milliQ water or PBS.

SPR experiments were performed to kinetically examine the importance of both lipid charge and the presence of the lipid bilayer on CP–lipid binding. In the presence of DMPG, CP displayed only a marginal dependence on the inner leaflet of the membrane bilayer (K_A bilayer/K_A monolayer = 1.92), but instead, relied more heavily on electrostatic interactions, presumably between CP's positively charged arginine and lysine residues and the anionic phospholipid head group of DMPG. Concerning CP interactions with zwitterionic DMPC bilayer membranes, besides presenting an approximately three-fold higher apparent K_A than that observed using DMPG bilayers, CP demonstrated a strong requirement for the hydrophobic interior provided by the lipid bilayer formed on the L1 sensor chip. This was observed by the lack of any observable peptide binding to DMPC monolayers (Figure 2(b)). As the bulky, positively charged choline head group of DMPC may have provided steric hindrance impeding CP interactions with the anionic phosphate groups of the phospholipids, the apparent driving force for this binding event was the presence of the lipid bilayer. The SPR results therefore suggest that while electrostatic interactions between CP and lipids are important for CP–lipid membrane binding, the presence of a membrane bilayer allows CP to bind with minimal peptide–lipid charge interactions.

To further characterize CP–lipid interactions, more specific models of peptide–lipid binding interactions, such as 1 : 1 Langmuir binding, parallel, and two-state reaction models were employed. In agreement with the currently accepted model for amphipathic peptide–lipid interactions [24,25,28,33], the two-state reaction model resulted in improved kinetic fits when compared to the alternate supplied models, but only for CP binding to DMPG bilayers. In this model, the membrane-insertion step defined by K_2 was found to approximate 1, at 0.92. This suggested that very little CP is permanently inserted into the membrane bilayer. However, this is in stark contrast to previous studies where it was shown that CP bound irreversibly to DMPC and DMPG lipid bilayers, likely within the hydrophobic interior of the lipid bilayer [17]. This discrepancy, in addition to the inability to obtain an acceptable fit using the two-state reaction model for CP interactions with DMPC bilayers, suggested that CP–lipid interactions are probably more complex than current models allow for. It may be that in this instance, the K_2 value may not represent the membrane-insertion step and that PL* (irreversibly bound peptide–lipid complex) represents a different binding intermediate. K_2 may therefore represent several steps occurring after the initial electrostatic interaction between CP and DMPG, such as possible peptide–peptide interactions occurring once bound to the lipid surface of the membrane but prior to membrane insertion. This may suggest a conformational change between lipid-associated CP molecules *prior* to membrane insertion as previously suggested [17].

Examination of CP secondary conformation resulting from the addition of increasing concentrations of lipid by CD suggested that lipids induce a conformational change dependent upon lipid charge (DMPG vs DMPC; anionic vs zwitterionic). The anionic DMPG altered CP conformation from a predominantly coil structure, to an almost exclusively β-structure in both milliQ water and PBS. The zwitterionic DMPC had little effect on CP conformation in either milliQ water or in PBS-based systems, further demonstrating the importance of charge in CP–lipid interactions [16,17,15,38].

It was interesting to note that while CP was derived from the presumed α-helical TM region of the TCR α-chain, CP was not shown to be helical in the presence of the lipids tested herein. One reason for this may be due to the difficulty in observing an α-helical spectra for a 9-amino acid peptide which may be present as a mixture of predominantly random, β-conformations or aggregates [37]. Another reason for the observed lack of α-helix may be due to the nature of the lipids tested. Presently, CP was tested in the presence of two different lipids, of which, one induced a predominantly β-conformation, while the other failed to induce any visible conformational change. It would be interesting to observe CP conformation in the presence of other lipids such as sphingomyelin, cholesterol, DMP-serine, or DMP-ethanolamine for examples.

Another interesting finding was the observation that in PBS, CP appeared to be aggregated. Currently, experiments are in progress to determine if this is in fact the case. These results may suggest that in ionic solutions such as PBS or cell culture media, CP (aggregates) may preferentially interact with anionic phospholipids (DMPG), as opposed to the zwitterionic DMPC phospholipids, on the cellular membrane.

Combining both SPR and CD results, data suggests that the initial binding of CP to lipid membranes is mediated by electrostatic interactions between the peptide and anionic lipids. Through hydrophobic interactions, CP may then insert into the membrane bilayer. In terms of a potential mode of action describing CP binding to T-cell membranes and the subsequent inhibition of T-cell activation at the level of the membrane bound TCR [12], *in vitro* experiments require that CP be prepared in media, which CD experiments in PBS suggest leads to CP aggregation. To overcome

DOI: 10.1002/psc

this, CP may preferentially interact with anionic lipids such as DMPG on the surface of the T-cells. While SPR suggests that this initial interaction is rapid, CD further suggests that this interaction may induce a conformational change in CP secondary structure. This structural change may then allow CP to insert into the membrane bilayer where some may remain irreversibly bound aided by the presence of zwitterionic lipids such as DMPC. Once within the membrane, CP may then be free to associate with membrane resident TCRs as suggested previously.

Acknowledgements

We express our sincere appreciation to Dr Maurits R. R. de Planque and Dr Alison Rodger for their expert advice on CD analysis, and Drs. Russell and Eve Diefenbach for helpful discussions on SPR analysis. We would also like to express our appreciation to Michael Apps for his help in CD data acquisition. Michael A. Amon is supported by scholarships from the National Health and Medical Research Council and the Barbara Cameron Memorial Scholarship, Sydney University. Marina Ali is supported by the Arthritis Foundation and a Henry Langley Fellowship. A grant-in-aid from the Rebecca Cooper Medical Research Foundation is appreciated.

REFERENCES

1. Call ME, Pyrdol J, Wiedmann M, Wucherpfennig KW. The organizing principle in the formation of the T cell receptor-CD3 complex. *Cell* 2002; **111**: 967–979.
2. Cosson P, Lankford SP, Bonifacino JS, Klausner RD. Membrane protein association by potential intramembrane charge pairs. *Nature* 1991; **351**: 414–416.
3. Engelman DM. Electrostatic fasteners hold the T cell receptor-CD3 complex together. *Mol. Cell.* 2003; **11**: 5–6.
4. Manolios N, Letourneur F, Bonifacino JS, Klausner RD. Pairwise, cooperative and inhibitory interactions describe the assembly and probable structure of the T-cell antigen receptor. *EMBO J.* 1991; **10**: 1643–1651.
5. Call ME, Wucherpfennig KW. The T Cell receptor: critical role of the membrane environment in receptor assembly and function. *Annu. Rev. Immunol.* 2005; **23**: 101–125.
6. Wang XM, Djordjevic JT, Bender V, Manolios N. T cell antigen receptor (TCR) transmembrane peptides colocalize with TCR, not lipid rafts, in surface membranes. *Cell Immunol.* 2002; **215**: 12–19.
7. Wang XM, Djordjevic JT, Kurosaka N, Schibeci S, Lee L, Williamson P, Manolios N. T-cell antigen receptor peptides inhibit signal transduction within the membrane bilayer. *Clin. Immunol.* 2002; **105**: 199–207.
8. Manolios N, Collier S, Taylor J, Pollard J, Harrison LC, Bender V. T-cell antigen receptor transmembrane peptides modulate T-cell function and T-cell mediated disease. *Nat. Med.* 1997; **3**: 84–88.
9. Manolios N, Huynh NT, Collier S. Peptides in the treatment of inflammatory skin disease. *Australas J. Dermatol.* 2002; **43**: 226–227.
10. Mahnke K, Qian Y, Jurgen K, Enk AH. Dendritic cells, engineered to secrete a T-cell receptor mimic peptide, induce antigen–specific immunosuppression in vivo. *Nat. Biotechnol.* 2003; **21**: 903–908.
11. Gollner G, Muller G, Alt R, Knop J, Enk AH. Therapeutic application of T cell receptor mimic peptides or cDNA in the treatment of T cell mediated skin diseases. *Gene Ther.* 2000; **7**: 1000–1004.
12. Amon MA, Ali M, Bender V, Chan Y-N, Toth I, Manolios N. Lipidation and glycosylation of a T-cell antigen receptor (TCR) transmembrane hydrophobic peptide dramatically enhances in vitro and in vivo function. *Biochim. Biophys. Acta* 2006; **1763**: 879–888.
13. Manolios N, Bonifacino JS, Klausner RD. Transmembrane helical interactions and the assembly of the T cell receptor complex. *Science* 1990; **249**: 274–277.
14. Huynh NT. T cell Antigen Receptor Transmembrane Peptides and their effects on B and Natural Killer Cells, University of Sydney, 2005.
15. Ali M, Amon M, Bender V, Manolios N. Hydrophobic transmembrane-peptide lipid conjugations enhance membrane binding and functional activity in T-cells. *Bioconjug. Chem.* 2005; **16**: 1556–1563.
16. Ali M, De Planque MRR, Huynh N, Manolios N, Separovic F. Biophysical studies of transmembrane peptide derived from the T cell antigen receptor. *Lett. Pept. Sci.* 2002; **8**: 227–233.
17. Bender V, Ali M, Amon M, Diefenbach E, Manolios N. T-cell antigen receptor peptide-lipid membrane interactions using surface Plasmon resonance. *J. Biol. Chem.* 2004; **279**: 54002–54007.
18. Bochicchio B, Pepe A, Tamburro AM. Circular dichroism studies on repeating polypeptide sequences of Abductin. *Chirality* 2005; **17**: 364–372.
19. Mangoni ML, Papo N, Mignogna G, Andreu D, Shai Y, Barra D, Simmaco M. Ranacyclins, a new family of short cyclic antimicrobial peptides: biological function, mode of action, and parameters involved in target specificity. *Biochemistry (Mosc.)* 2003; **42**: 14023–14035.
20. Avrahami D, Shai Y. Conjugation of a magainin analogue with lipophilic acids controls hydrophobicity, solution assembly, and cell selectivity. *Biochemistry (Mosc.)* 2002; **41**: 2254–2263.
21. Mozsolits H, Unabia S, Ahmad A, Morton CJ, Thomas WG, Aguilar M-I. Electrostatic and hydrophobic forces tether the proximal region of the angiotensin II receptor (AT_{1A}) carboxyl terminus to anionic lipids. *Biochemistry (Mosc.)* 2002; **41**: 7830–7840.
22. Najbar LV, Craik DJ, Wade JD, McLeish MJ. Identification of initiation sites for T4 lysozyme folding using CD and NMR spectroscopy of peptide fragments. *Biochemistry (Mosc.)* 2000; **39**: 5911–5920.
23. Najbar LV, Craik DJ, Wade JD, Salvatore D, McLeish MJ. Conformational analysis of LYS(11–36), a peptide derived from the b-sheet region of T4 lysozyme, in TFE and SDS. *Biochemistry (Mosc.)* 1997; **36**: 11525–11533.
24. Papo N, Shai Y. Exploring peptide membrane interaction using surface plasmon resonance: Differentiation between pore formation versus membrane disruption by lytic peptides. *Biochemistry (Mosc.)* 2003; **42**: 458–466.
25. Mozsolits H, Aguilar M-I. Surface Plasmon resonance spectroscopy: An emerging tool for the study of peptide-membrane interactions. *Biopolymers (Pept. Sci.)* 2002; **66**: 3–18.
26. Mozsolits H, Wirth HJ, Werkmeister J, Aguilar M-I. Analysis of antimicrobial peptide interactions with hybrid bilayer membrane systems using surface plasmon resonance. *Biochim. Biophys. Acta* 2001; **1512**: 64–76.
27. Lee T-H, Mozsolits H, Aguilar M-I. Measurement of the affinity of melittin for zwitterionic and anionic membranes using immobilized lipid biosensors. *J. Pept. Res.* 2001; **58**: 464–476.
28. Mozsolits H, Lee T-H, Clayton AHA, Sawyer WH, Aguilar M-I. The membrane-binding properties of a class A amphipathic peptide. *Eur. Biophys. J.* 2004; **33**: 98–108.
29. Jin Y, Mozsolits H, Hammer J, Zmuda E, Zhu F, Zhang Y, Aguilar MI, Blazyk J. Influence of tryptophan on lipid binding of

linear amphipathic cationic antimicrobial peptides. *Biochemistry (Mosc.)* 2003; **42**: 9395–9405.
30. Kamimori H, Hall K, Craik DJ, Aguilar M-I. Studies on the membrane interactions of the cyclotides kalata B1 and kalata B6 on model membrane systems by surface plasmon resonance. *Anal. Biochem.* 2005; **337**: 149–153.
31. Suh W-C, Lu CZ, Gross CA. Structural features required for the interaction of the Hsp70 molecular chaperone DnaK with its cochaperone DnaJ. *J. Biol. Chem.* 1999; **274**: 30534–30539.
32. Reed J, Reed TA. A set of constructed type spectra for the practical estimation of peptide structure from circular dichroism. *Anal. Biochem.* 1997; **254**: 36–40.
33. Karlsson R, Falt A. Experimental design for kinetic analysis of protein-protein interactions with surface plasmon resonance biosensors. *J. Immunol. Methods* 1997; **200**: 121–133.
34. Saenko E, Sarafanov A, Ananyeva N, Behre E, Shima M, Schwinn H, Josic D. Comparison of the properties of phospholipid surfaces formed on HPA and L1 biosensor chips for the binding of coagulation factor VIII. *J. Chromatogr. A* 2001; **921**: 49–56.
35. Whitmore L, Wallace BA. DICHROWEB, an online server for protein secondary structure analyses from circular dichroism. *Nucleic Acids Res.* 2004; **32**: w668.
36. Wang XM. *Biological and Biophysical Properties of T-cell Antigen Receptor (TCR) Transmembrane Peptides in Cell Membranes*. University of Sydney: Sydney, 2001.
37. Gerber D, Quintana FJ, Bloch I, Cohen IR, Shai Y. D-enantiomer peptide of the TCRα transmembrane domain inhibits T-cell activation in vitro and in vivo. *FASEB J.* 2005; **19**: 1190–1192.
38. Ali M, Salam NK, Amon MA, Bender V, Hibbs DE, Manolios N. T-cell antigen receptor–alpha chain transmembrane peptides: Correlation between structure and function. *Int. J. Pept. Res. Therap.* 2006; **12**: 261–267.